SF2A 2025
A. Siebert, K. Baillié, M. Béthermin, F. Cantalloube, E. Josselin, N. Lagarde, J. Malzac, J. Richard, L. Selliez, O. Venot (eds)

NOEMA ASTROCHEMISTRY OF CYGNUS-X PROTOSTARS (NASCENT-STARS)

T. Csengeri[1], L. Bouscasse[2], D. Panda[1], N. Kessler[1] and NASCENT-stars collaboration

Abstract. During the star formation process, the interstellar medium gets enriched in a complex zoo of molecules, potentially establishing a molecular heritage for the chemistry of disks and their forming planetary systems. It is, however, unclear what are the key physical conditions that influence the emerging complex chemistry, and how the fundamental properties of the emerging star, or stellar clusters impact the chemical evolution. Wide-band spectral surveys are powerful tools to provide reliable molecular abundance estimates. Combined with an interferometric resolving power they can reach and resolve the scale of individual collapsing envelopes and give insight into both the physical and chemical evolution of the gas taking place in the star formation process. The NASCENT-stars large observing program at NOEMA performs a sensitive interferometric unbiased spectral line survey of the most active star forming massive dense cores in the Cygnus-X complex. We aim to characterise the physico-chemical conditions at $\sim$1400 au scales using a 46.5 GHz non-continuous, dual-band observing strategy. This provides us reliable measurements of molecular abundances towards statistically significant samples of individual protostellar envelopes.

Keywords: Stars: formation, ISM: molecules, Submillimeter: ISM, Astrochemistry

1 Introduction

The chemical evolution during star formation leads to the emergence of complex organic molecules (COMs) that includes sugars, alcohols, aldehydes, and prebiotic molecules, which are key to the emergence of life (see e.g. Jørgensen et al. 2020; Jimenez-Serra et al. 2025). Constraining the key processes leading to this chemical enrichment is the first step to understand the potential molecular inheritance of star formation to the early chemical evolution of protoplanetary disks.

Using sufficiently wide-band spectral coverage with transitions from a large range of upper level energies allows us to characterise chemically rich regions. The physical conditions of the emitting gas can be inferred from modelling, typically using Local Thermodynamic Equilibrium (LTE) assumption. This allows us to infer molecular column density ($N_{\rm X}$), the gas kinetic temperature ($T_{\rm kin}$), and gas kinematics, such as the turbulent and thermal line-width (Δv), and the source rest velocity ($v_{\rm lsr}$). The continuum background emission can be measured, and ideally the size of the emitting region needs to be known (Θ). Overall this allows us to elucidate the physical properties of the emitting gas, together with its molecular composition. Molecular abundances are typically estimated relative to H_2, or other species where the column densities are well constrained (such as CH_3OH, HNCO, or other species).

Observations of COMs towards low- and high-mass star forming regions suggest similar trends in molecular abundances, at least for certain O-bearing COMs (Coletta et al. 2020; Nazari 2025), suggesting that the chemical processes taking place in the star forming gas are rather similar over a wide range of physical conditions. This is somewhat contradictory to observations of chemical differentiation that is confirmed towards low- and high-mass envelopes, because it suggests that the local physical conditions greatly impact the structuration and the localisation of molecules that would lead to molecular abundances greatly dependent on the local conditions. Consequently, significant questions remain open, such as how the abundance and diversity of COMs depend on physical properties like protostar mass and age, and how environmental factors and physical processes such as radiative heating and shocks influence molecular complexity. Statistical samples of well constrained molecular abundances are required to answer these questions. The principal goal of the NASCENT-stars large program is to obtain such reliable molecular abundances for a large number of protostellar envelopes. Here we aim to introduce this observing program and present a brief highlight of its preliminary results.

[1] Laboratoire d'Astrophysique de Bordeaux, Univ. Bordeaux, CNRS, LAB, UMR 5804, F-33600 Pessac, France
[2] IRAM

2 Target selection in the Cygnus-X molecular complex

Located at a 1.4 kpc distance (Rygl et al. 2012), the Cygnus-X molecular cloud offers a unique region to investigate star and cluster formation including the formation of accompanying intermediate to high-mass stars. It has been extensively studied in molecular lines (e.g. Schneider et al. 2006; Imanaly et al. 2025), thermal dust emission (e.g. Motte et al. 2007, 2010; Roy et al. 2011; Hennemann et al. 2012; Schneider et al. 2016; Cao et al. 2021), radio emission (Downes & Rinehart 1966; Ortiz-León et al. 2021), as well as several optical and infrared studies (e.g. Beerer et al. 2010; Wright et al. 2010; Kryukova et al. 2014; Román-Zúñiga et al. 2023). The region contains an estimated gas mass of $\sim 1-4\times10^6$ $M_\odot$ available for star formation (Schneider et al. 2006; Zhang et al. 2024), and a sample of massive dense cores (MDCs) has been identified by Motte et al. (2007) using IRAM 30m/MAMBO observations.

Towards a sample of MDCs, precursors of high-mass stars and their dynamically forming clusters have been identified with the Plateau de Bure interferometer reaching scales of ∼2000–4000 au (Bontemps et al. 2010; Csengeri et al. 2011). Using primarily CO (J=2–1) emission Duarte-Cabral et al. (2013) identified their associated molecular outflow emission pinpointing star forming activity. These studies suggest that 0.05–0.1 pc scale MDCs fragment and host compact sources at <2000 au. On the other hand, these envelopes do not appear to be subfragmented down to ∼500 au scales (Fechtenbaum 2015, Panda et al. in prep). Observations reaching <2000 au physical resolution are therefore required to study individual collapsing envelopes. Intermediate scales at ∼5000 au have been covered by the complementary CASCADE large program (in the frame of Max-Planck IRAM Observatory Program) using NOEMA C+D configurations in the 3mm band (Beuther et al. 2022).

Herschel observations from the HOBYS program (Motte et al. 2010) provide a complete overview of the most prominent dense gas regions corresponding to MDCs, and deliver dust based physical properties, such as dust temperature, mass and bolometric luminosity. This information was combined with the list of MDCs identified in Motte et al. (2007), from which we selected a representative sample of 17 MDCs corresponding to sources with mass > 30 $M_\odot$ and luminosities of $< 10^4$ $L_\odot$. Our source selection includes two of the most prominent and young star forming sites, DR21(OH) and W75N, otherwise we aimed to avoid the most luminous HII regions where strong ionising radiation may already start to destroy molecules.

3 Observations

NASCENT-stars is a large observing program at the IRAM* NOEMA interferometer (Project id: L23AA, PI: Csengeri). It makes use of its enhanced sensitivity and spectral resolution, and exploits the 250 kHz observing mode of the Polyfix correlator. We perform three spectral setups to obtain a dual-band, non-continuous spectral coverage of ∼46.5 GHz.

Two setups cover a continuous frequency range between ∼84 and 115.5 GHz corresponding to a significant part of the 3mm atmospheric transmission window. Another setup in the 1mm atmospheric transmission window is used to cover the 213.9–221.6 GHz and 229.4–237.1 GHz frequency ranges. To foster synergy with other large observing programs, this setup covers the transitions observed with the ALMA-IMF large program (Motte et al. 2022; Ginsburg et al. 2022), while due to its unbiased approach the 3mm setup inherently covers all ALMA-IMF setups in that band. We obtain a velocity resolution of 0.7-0.9 km s^{-1} in the 3mm band, and ∼0.3 km s^{-1} in the 1mm band. Single-pointing observations are used for the 3mm setups combining A and C configurations with track sharing. For the 1mm setup, we use the A configuration and perform small mosaics with 13 pointings to map out the primary beam of the 3mm pointed observations at a homogeneous sensitivity. The observations were carried out in the new track sharing mode. The resulting synthesised beam with natural weighting is ∼1" (1400 au) for both bands. Observations for the large program have started in 2023 at NOEMA and are, as of now, still on-going.

Complementary short spacings information has been obtained with the IRAM 30m telescope in order to recover emission from spatial scales filtered out by NOEMA (Project id: 064-23). The EMIR receiver has similar observed bandwidth (Carter et al. 2012), and the FTS backends provide a 200 kHz spectral resolution.

*IRAM is supported by INSU/CNRS (France), MPG (Germany), and IGN (Spain).

4 First results

4.1 3mm continuum emission

We show here results from observations targeting the CygX-N53 MDC, and focus on the 3mm dataset that has been observed as a pilot projet (W21AS) with a 62.5 kHz setup, instead of the 250 kHz of the large program (a more exhaustive description of the observations is given in a forthcoming paper by Csengeri et al. *in prep*). The observations shown here have been carried out using the old A configuration, corresponding to the current B configuration of NOEMA resulting in a somewhat larger synthesized beam of about 1.″3. Figure 1 (left) shows the obtained line-free continuum image, where emission between 82 and 113 GHz has been averaged assuming a flat spectral index. It demonstrates that we resolve individual envelopes. Comparing with old CD configuration data from the Plateau de Bure Interferometer by Bontemps et al. (2010), our NOEMA observations achieve a clearly better sensitivity at a $\sim 3\times$ higher angular resolution. The global morphology of the 3mm continuum emission remains, however, very similar to previous observations, and resembles closely the 1mm band image of Bontemps et al. (2010), with similar angular resolution as the here presented new data.

Overall, the CygX-N53 region is characterised by two bright and closely located continuum peaks dominating the emission with other lower intensity companions located in their immediate vicinity. Due to the increased sensitivity, a large number of fainter compact sources also appear dispersed over the map. In addition to the CygX-N53 MDC of Motte et al. (2007), we also detect compact sources associated with the MDC CygX-N54 (W75S-FIR3) located southwest from the phase center, and CygX-N52 that is located north from the phase center. These sources are labeled in Fig. 1 (left), and have an important contribution to the overall continuum emission. We perform source extraction using a Gaussian source finding algorithm as well as identifying compact sources in a Laplacian transformation of the emission maps. The results will be presented in a forthcoming paper by Panda et al. (in prep). Overall the conclusion is that we identify about 25 sources in contrast to the 7 sources identified by Bontemps et al. (2010). Compared to these previous studies, we significantly increase the number of known compact continuum sources in the region. This allows us to conclude that with the requested continuum sensitivity we are able to obtain a large statistics of compact cores from the low- to high-mass regime. Extrapolating to all 17 observed fields, we expect to find about 60 high-mass envelopes.

4.2 3mm frequency coverage

We illustrate the frequency coverage of the pilot dataset in Fig. 1 (right). This is shifted by about 2 GHz compared to that of the large program, and has been optimised based on the pilot observations. Since no bright emission lines are seen in the 82–84 GHz range, for the large program we shifted the frequency coverage to include the CO (J=1–0) transition instead. Combined with the CO (J=2–1) transition covered in the 1mm observations, this will allow us to perform quantitative studies of the excitation conditions in the outflowing gas.

The shown spectrum corresponds to that of the brightest millimeter core, MM1 in Bontemps et al. (2010). We tested our recently developed CNN-based line analysis algorithm (Kessler et al. 2025) that provided us a preliminary list of species present in the spectrum. We notice emission lines from several COMs, including that of CH_3OH, CH_3OCHO, CH_3OCH_3 that is a non exhaustive list of the detected COM emission. Proper LTE modelling of the observed spectrum is currently on-going.

5 Conclusions and outlook

First results of NASCENT-stars demonstrate that our requested sensitivity is sufficient to reach the sub-solar mass envelope range within forming clusters. We also show that emission from COMs is detected in the 3mm band observations. Extrapolating these results to the full sample, this observing program will deliver the statistically significant sample of pre-/protostellar envelopes to study the process of star formation at ∼1400 au scales towards selected regions of the Cygnus-X molecular cloud.

Furthermore, emission from several COMs is detected towards the brightest, i.e. most massive protostellar envelopes. However, we expect observations in the 1mm band to be more sensitive to the compact hot gas component and thus be able to trace the population of low- and intermediate-mass chemically rich sites corresponding to hot corinos. Line stacking could further increase our sensitivity to detect COM emission from the weakest sources.

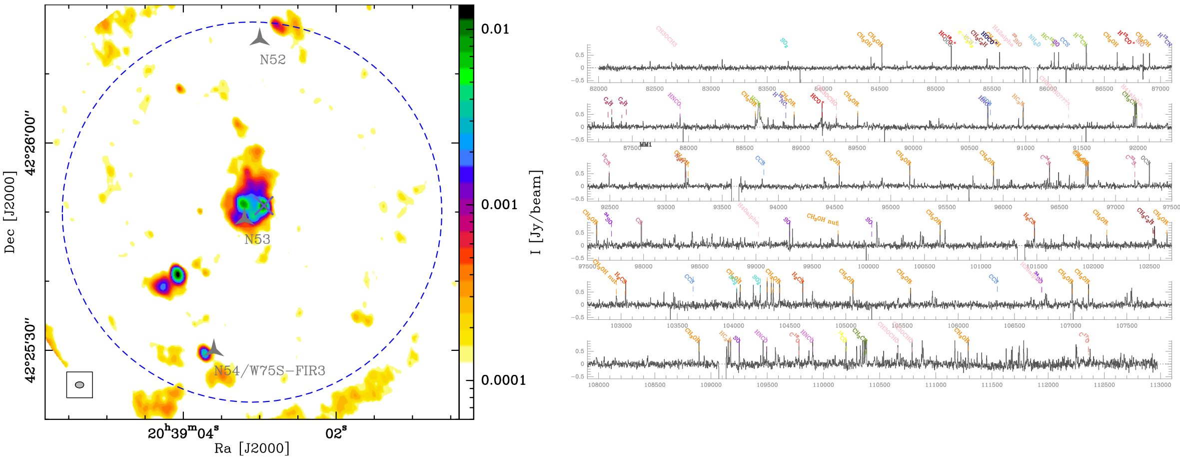

Fig. 1. Left: 3mm continuum emission of the CygX-N53 MDC, the scaling is logarithmic between 0.02 and 13.8 mJy/beam. The blue dashed ellipse shows a 55" primary beam. The synthesised beam is shown in the lower left corner. The positions of the MDCs from Motte et al. (2007) corresponding to emission peaks at 1.2 mm are marked and labeled in grey. **Right:** Spectrum extracted towards the MM1 continuum peak. Transitions from abundant species are labeled in color.

With the NASCENT-stars large program our aim is to obtain precise molecular abundance estimates at the scale of individual protostellar envelopes reaching scales of about 1400 au. We expect to detect emission from COMs for over >60 protostellar envelopes covering the intermediate to the high-mass range allowing us to statistically study molecular abundances and spatial differentiation of species in a systematic way. This offers a comprehensive view of molecular content and the chemical evolution of star-forming gas. Simultaneously capturing low-, intermediate- and high-mass envelopes, this project will also explore whether chemical similarities between hot cores and hot corinos indicate common processes in COM formation. Additionally, spatial differentiation between O- and N-bearing COMs, as observed in intermediate- and high-mass envelopes, will be further investigated. These efforts will provide a detailed understanding of the chemical and physical properties of protostellar envelopes and set constraints on the production channels of COMs, whether through grain surface or gas-phase chemistry. By combining the results with advanced models, we expect this study to significantly advance our understanding of the chemical evolution during star formation.

References

Beerer, I. M., Koenig, X. P., Hora, J. L., et al. 2010, ApJ, 720, 679

Beuther, H., Wyrowski, F., Menten, K. M., et al. 2022, A&A, 665, A63

Bontemps, S., Motte, F., Csengeri, T., & Schneider, N. 2010, A&A, 524, A18

Cao, Y., Qiu, K., Zhang, Q., Wang, Y., & Xiao, Y. 2021, ApJ, 918, L4

Carter, M., Lazareff, B., Maier, D., et al. 2012, A&A, 538, A89

Coletta, A., Fontani, F., Rivilla, V. M., et al. 2020, A&A, 641, A54

Csengeri, T., Bontemps, S., Schneider, N., Motte, F., & Dib, S. 2011, A&A, 527, A135

Downes, D. & Rinehart, R. 1966, ApJ, 144, 937

Duarte-Cabral, A., Bontemps, S., Motte, F., et al. 2013, A&A, 558, A125

Fechtenbaum, S. 2015, PhD thesis, Universite de Bordeaux, Talence, France

Ginsburg, A., Csengeri, T., Galván-Madrid, R., et al. 2022, A&A, 662, A9

Hennemann, M., Motte, F., Schneider, N., et al. 2012, A&A, 543, L3

Imanaly, E., Esimbek, J., Baan, W., et al. 2025, MNRAS, 542, 2074

Jimenez-Serra, I., Codella, C., & Belloche, A. 2025, arXiv e-prints, arXiv:2503.17104

Jørgensen, J. K., Belloche, A., & Garrod, R. T. 2020, ARA&A, 58, 727

Kessler, N., Csengeri, T., Cornu, D., Bontemps, S., & Bouscasse, L. 2025, subm

Kryukova, E., Megeath, S. T., Hora, J. L., et al. 2014, AJ, 148, 11
Motte, F., Bontemps, S., Csengeri, T., et al. 2022, A&A, 662, A8
Motte, F., Bontemps, S., Schilke, P., et al. 2007, A&A, 476, 1243
Motte, F., Zavagno, A., Bontemps, S., et al. 2010, A&A, 518, L77
Nazari, P. 2025, arXiv e-prints, arXiv:2508.15771
Ortiz-León, G. N., Menten, K. M., Brunthaler, A., et al. 2021, A&A, 651, A87
Panda, D., Csengeri, T., & Bouscasse, L. in prep
Román-Zúñiga, C. G., Kounkel, M., Hernández, J., et al. 2023, AJ, 165, 51
Roy, A., Ade, P. A. R., Bock, J. J., et al. 2011, ApJ, 727, 114
Rygl, K. L. J., Brunthaler, A., Sanna, A., et al. 2012, A&A, 539, A79
Schneider, N., Bontemps, S., Motte, F., et al. 2016, A&A, 591, A40
Schneider, N., Bontemps, S., Simon, R., et al. 2006, A&A, 458, 855
Wright, N. J., Drake, J. J., Drew, J. E., & Vink, J. S. 2010, ApJ, 713, 871
Zhang, S., Su, Y., Chen, X., et al. 2024, AJ, 167, 220